



A simple approach for finite element simulation of reinforced plates

Erik Burman^a, Peter Hansbo^{b,*}, Mats G. Larson^c

^a Department of Mathematics, University College London, London, UK–WC1E 6BT, United Kingdom

^b Department of Mechanical Engineering, Jönköping University, S-551 11, Jönköping, Sweden

^c Department of Mathematics and Mathematical Statistics, Umeå University, SE-901 87, Umeå, Sweden

ARTICLE INFO

Keywords:

Cut finite element method
Discontinuous Galerkin
Kirchhoff–Love plate
Euler–Bernoulli beam
Reinforced plate

ABSTRACT

We present a new approach for adding Bernoulli beam reinforcements to Kirchhoff plates. The plate is discretised using a continuous/discontinuous finite element method based on standard continuous piecewise polynomial finite element spaces. The beams are discretised by the CutFEM technique of letting the basis functions of the plate represent also the beams which are allowed to pass through the plate elements. This allows for a fast and easy way of assessing where the plate should be supported, for instance, in an optimization loop.

1. Introduction

Reinforcements of plates using lower-dimensional structures such as beams are often employed for the purpose of increasing buckling loads and avoiding eigenfrequencies in vibration problems. The effect of stiffeners can be simulated in a finite element context in a variety of ways. The important issue is how to couple the variables of the beam to the variables of the plate. Different approaches have been suggested:

- Point (nodal) constraints matching beam and plate displacements [20].
- Lagrange multipliers to tie the beam and plate [17].
- Using the plate basis functions also for the beam, along edges or aligned with the elements [5], or obliquely [13,16,19].

The last approach has only been used in the context of Timoshenko beams coupled to Mindlin–Reissner plates, where simple C^0 approximations can be used; a similar approach was recently suggested for modeling embedded trusses by Lé, Legrain, and Moës [15]. In this paper we present a method for the coupling of Kirchhoff plates and Euler–Bernoulli beams based on this concept, together with a tangential differential approach which simplifies the implementation for arbitrarily oriented beams. This is possible thanks to the development of continuous/discontinuous Galerkin (c/dG) methods for higher order problems [6,7,9,10], avoiding the use of C^1 -continuity.

The fact that we do not have to employ higher continuity allows for coupling in other contexts as well. In Ref. [12] we proposed to use the same finite element space for the beam as for the higher dimensional

structure modeled by linear elasticity, using second order polynomials for elasticity and taking the restriction, or trace, of these polynomials to model the beam using c/dG.

2. Modeling of reinforced plates

2.1. The basic approach

In this Section we develop a simple model of a set of beam elements in a plate. The main approach is as follows:

- Given a continuous finite element space, based on at least second order polynomials for the plate, we define the finite element space for the one-dimensional structure as the restriction of the plate finite element space to the structure which is geometrically modeled by an embedded curve or line.
- To formulate a finite element method on the restricted or trace finite element space we employ continuous/discontinuous Galerkin approximations of the Euler–Bernoulli beam model. The beams are then modeled using the CutFEM paradigm and the stiffness of the embedded beams is in the most basic version, which we consider here, simply added to the plate stiffness.

To ensure coercivity of the cut beam model we in general need to add a certain stabilization term which provides control of the discrete functions variation in the vicinity of the beam. However, for beams embedded in a plate, the plate stabilizes the beam discretizations, and

* Corresponding author.

E-mail address: peter.hansbo@ju.se (P. Hansbo).

we shall show that if the plate is stiff enough compared to the beam the usual additional stabilization [1] is superfluous. The plate problem may also be viewed as an interface problem in order to more accurately approximate the plate in the vicinity of the beam structure; this approach is however significantly more demanding from an implementation point of view and we leave it for future work.

The work presented here is an extension of earlier work [4] where membrane structures were considered, in which case a linear approximation in the bulk suffices.

2.2. The Kirchhoff–Love plate model

In the Kirchhoff–Love plate model, posed on a polygonal domain $\Omega \subset \mathbb{R}^2$ with boundary $\partial\Omega$ and exterior unit normal $\mathbf{n}_{\partial\Omega}$, we seek an out-of-plane (scalar) displacement u to which we associate the strain (curvature) tensor

$$\epsilon(\nabla u) := \frac{1}{2} (\nabla \otimes (\nabla u) + (\nabla u) \otimes \nabla) = \nabla \otimes \nabla u = \nabla^2 u \quad (1)$$

and the plate stress (moment) tensor

$$\sigma_p(\nabla u) := C_p (\epsilon(\nabla u) + \nu_\Omega (1 - \nu_\Omega)^{-1} \text{div} \nabla u \mathbf{I}) \quad (2)$$

$$= C_p (\nabla^2 u + \nu_\Omega (1 - \nu_\Omega)^{-1} \Delta u \mathbf{I}) \quad (3)$$

where

$$C_p = \frac{E_\Omega t_\Omega^3}{12(1 + \nu_\Omega)} \quad (4)$$

with E_Ω the Young’s modulus, ν_Ω the Poisson’s ratio, and t_Ω denotes the plate thickness. Since $0 \leq \nu_\Omega \leq 0.5$ the constants are uniformly bounded.

The Kirchhoff–Love problem then takes the form: given the out-of-plane load (per unit area) f , find the displacement u such that

$$\text{div} \text{div} \sigma_p(\nabla u) = f \quad \text{in } \Omega \quad (5)$$

$$u = 0 \quad \text{on } \partial\Omega \quad (6)$$

$$\mathbf{n}_{\partial\Omega} \cdot \nabla u = 0 \quad \text{on } \partial\Omega \quad (7)$$

where div and div denote the divergence of a tensor and a vector field, respectively.

Weak Form. The variational problem takes the form: Find the displacement $u \in V_\Omega = H_0^2(\Omega)$ such that

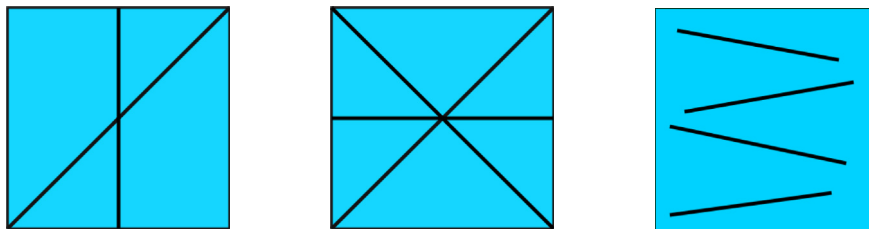


Fig. 1. Examples of plates reinforced by beams.

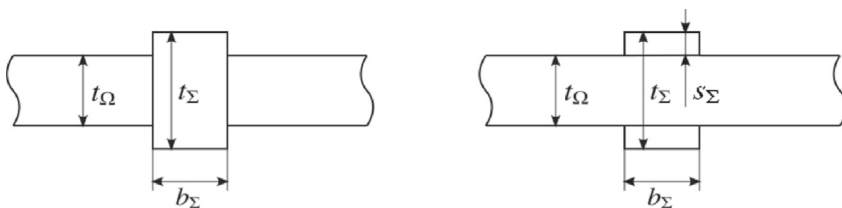


Fig. 2. Left: The reinforced plate geometry parameters, t_Ω , t_Σ , and b_Σ . Right: Alternative design of reinforcement with two separate beams of thickness $s_\Sigma = (t_\Sigma - t_\Omega)/2$ above and below the plate.

$$a_\Omega(u, v) = l_\Omega(v) \quad \forall v \in V_\Omega \quad (8)$$

where the forms are defined by

$$a_\Omega(v, w) = (\sigma_p(\nabla v), \epsilon(\nabla w))_\Omega \quad (9)$$

$$l_\Omega(v) = (f, v)_\Omega \quad (10)$$

We employ the following notation: $L^2(\omega)$ is the Lebesgue space of square integrable functions on ω with scalar product $(\cdot, \cdot)_{L^2(\omega)} = (\cdot, \cdot)_\omega$ and $\|\cdot\|_{L^2(\omega)} = \|\cdot\|_\omega$ and $\|\cdot\|_{L^2(\Omega)} = \|\cdot\|$, $H^s(\omega)$ is the Sobolev space of order s on ω with norm $\|\cdot\|_{H^s(\omega)}$, and $H_0^1(\Omega) = \{v \in H^1(\Omega) : v = 0 \text{ on } \partial\Omega\}$, and $H_0^2(\Omega) = \{v \in H^2(\Omega) : v = \mathbf{n}_{\partial\Omega} \cdot \nabla v = 0 \text{ on } \partial\Omega\}$.

2.3. The Euler–Bernoulli beam model

Consider a straight thin beam with centerline $\Sigma \subset \Omega$ and a rectangular cross-section with width b_Σ and thickness t_Σ , see Fig. 2. The modeling of the beam is performed using tangential differential calculus and we follow the exposition in Refs. [11,12], which also covers curved beams. Using this approach the beam equation is expressed in the same coordinate system as the plate, which is convenient in the construction of the cut finite element method for reinforced plates, see Fig. 1 for examples.

Let \mathbf{t} be the tangent vector to the line Σ and $\mathbf{P}_\Sigma = \mathbf{t} \otimes \mathbf{t}$ the projection onto the one dimensional tangent space of Σ and define the tangential derivatives

$$\nabla_\Sigma v = \mathbf{P}_\Sigma \nabla v, \quad \partial_t v = \mathbf{t} \cdot \nabla v \quad (11)$$

Then we have the identity

$$\nabla_\Sigma v = (\partial_t v) \mathbf{t} \quad (12)$$

Based on the assumption that planar cross sections orthogonal to the midline remain plane after deformation we assume that the displacement takes the form

$$u = u\mathbf{n} + \theta \zeta \mathbf{t} \quad (13)$$

where ζ is the signed orthogonal distance to Ω , positive on one side of Ω and negative on the other side, and $\theta : \Sigma \rightarrow \mathbb{R}$ is an angle representing an infinitesimal rotation, assumed constant in the normal plane.

In Euler–Bernoulli beam theory the beam cross-section is assumed plane and orthogonal to the beam midline after deformation and no shear deformations occur, which means that we have

$$\theta = \mathbf{t} \cdot \nabla u := \partial_t u \quad (14)$$

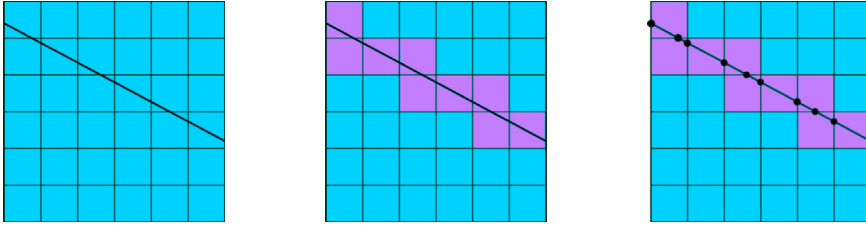


Fig. 3. The mesh \mathcal{T}_h with one beam, the active mesh $\mathcal{T}_h(\Sigma)$ for the beam in purple, and the set of intersection points $\mathcal{P}_h(\Sigma)$. (For interpretation of the references to colour in this figure legend, the reader is referred to the Web version of this article.)

This definition for θ in combination with (13) constitutes the Euler–Bernoulli kinematic assumption

$$\mathbf{u} = \mathbf{u}\mathbf{n} + \zeta(\partial_t \mathbf{u})\mathbf{t} = \mathbf{u}\mathbf{n} + \zeta \nabla_\Sigma \mathbf{u}$$

We assume the usual Hooke’s law for one dimensional structural members

$$\boldsymbol{\sigma}_\Sigma(\mathbf{u}) = E_\Sigma \boldsymbol{\varepsilon}_\Sigma(\mathbf{u}) \quad (15)$$

where E_Σ is the Young modulus and the tangential strain tensor is given by

$$\boldsymbol{\varepsilon}_\Sigma(\mathbf{u}) = \mathbf{P}_\Sigma \boldsymbol{\varepsilon}(\mathbf{u}) \mathbf{P}_\Sigma = \zeta \boldsymbol{\varepsilon}_\Sigma(\nabla_\Sigma \mathbf{u}) \quad (16)$$

where in the last equality we used the identity

$$\mathbf{u} \otimes \nabla = (\mathbf{u}\mathbf{n} + \zeta \nabla_\Sigma \mathbf{u}) \otimes \nabla = \mathbf{n} \otimes (\nabla \mathbf{u}) + \zeta (\nabla_\Sigma \mathbf{u}) \otimes \nabla \quad (17)$$

to conclude that

$$\boldsymbol{\varepsilon}_\Sigma(\mathbf{u}) = \zeta \boldsymbol{\varepsilon}_\Sigma(\nabla_\Sigma \mathbf{u}) \quad (18)$$

Next note that the strain energy density can be written

$$\boldsymbol{\sigma}_\Sigma(\mathbf{u}) : \boldsymbol{\varepsilon}_\Sigma(\mathbf{u}) = \zeta^2 \boldsymbol{\sigma}_\Sigma(\nabla_\Sigma \mathbf{u}) : \boldsymbol{\varepsilon}(\nabla_\Sigma \mathbf{u}) \quad (19)$$

and the total energy of the beam structure is obtained by integrating over the beam volume

$$\mathcal{E}_\Sigma = \frac{1}{2} \int_\Sigma I_\Sigma \boldsymbol{\sigma}_\Sigma(\nabla_\Sigma \mathbf{u}) : \boldsymbol{\varepsilon}(\nabla_\Sigma \mathbf{u}) \, d\Sigma - \int_\Sigma a_\Sigma f_\Sigma \mathbf{u} \, d\Sigma \quad (20)$$

where the integral over the cross section is accounted for by the cross-section area and its second moment

$$a_\Sigma = b_\Sigma t_\Sigma, \quad I_\Sigma = b_\Sigma t_\Sigma^3 / 12 \quad (21)$$

We are thus led to introducing the beam stress tensor

$$\boldsymbol{\sigma}_{B,\Sigma}(\nabla_\Sigma \mathbf{v}) = I_\Sigma \boldsymbol{\sigma}_\Sigma(\nabla_\Sigma \mathbf{v}) = I_\Sigma E_\Sigma \boldsymbol{\varepsilon}_\Sigma(\nabla_\Sigma \mathbf{v}) \quad (22)$$

and thus we have the beam Hooke law

$$\boldsymbol{\sigma}_{B,\Sigma}(\nabla_\Sigma \mathbf{v}) = C_B \boldsymbol{\varepsilon}_\Sigma(\nabla_\Sigma \mathbf{v}) \quad (23)$$

where

$$C_B = E_\Sigma I_\Sigma = \frac{E_\Sigma b_\Sigma t_\Sigma^3}{12} \quad (24)$$

Taking variations we obtain the weak statement, assuming zero displacements and rotations at the end points of Σ , we thus seek $u \in V_\Sigma = H_0^2(\Sigma)$, such that

$$a_\Sigma(u, v) = l_\Sigma(v) \quad \forall v \in V_\Sigma \quad (25)$$

where the forms are defined by

$$a_\Sigma(v, w) = \int_\Sigma \boldsymbol{\sigma}_{B,\Sigma}(\nabla_\Sigma \mathbf{v}) : \boldsymbol{\varepsilon}_\Sigma(\nabla_\Sigma \mathbf{w}) \, d\Sigma, \quad l_\Sigma(v) = \int_\Sigma a_\Sigma f_\Sigma v \, d\Sigma \quad (26)$$

Remark 1. We have the identity

$$\boldsymbol{\varepsilon}_\Sigma(\nabla_\Sigma \mathbf{v}) = (\partial_t^2 \mathbf{v}) \mathbf{t} \otimes \mathbf{t} \quad (27)$$

since $(\nabla_\Sigma \mathbf{v}) \otimes \nabla_\Sigma = ((\partial_t \mathbf{v}) \mathbf{t}) \otimes \nabla_\Sigma = (\partial_t (\partial_t \mathbf{v}) \mathbf{t}) \otimes \mathbf{t} = (\partial_t^2 \mathbf{v}) \mathbf{t} \otimes \mathbf{t}$, where $\partial_t (\partial_t \mathbf{v}) = \partial_t^2 \mathbf{v}$ since \mathbf{t} is constant, which leads to

$$\boldsymbol{\sigma}_{B,\Sigma}(\nabla_\Sigma \mathbf{v}) : \boldsymbol{\varepsilon}(\nabla_\Sigma \mathbf{w}) = E_\Sigma I_\Sigma \partial_t^2 v \partial_t^2 w \quad (28)$$

which leads to

$$a_\Sigma(v, w) = \int_\Sigma \boldsymbol{\sigma}_{B,\Sigma}(\nabla_\Sigma \mathbf{v}) : \boldsymbol{\varepsilon}(\nabla_\Sigma \mathbf{w}) \, d\Sigma = \int_\Sigma E_\Sigma I_\Sigma \partial_t^2 v \partial_t^2 w \, d\Sigma \quad (29)$$

Here we recognize the right hand side as the traditional bilinear form associated with the Euler–Bernoulli beam.

Remark 2. We note that in the alternative reinforcement geometry, right in Fig. 2, we have

$$a_\Sigma = b_\Sigma (t_\Sigma - t_\Omega), \quad I_\Sigma = \frac{E_\Sigma b_\Sigma (t_\Sigma^3 - t_\Omega^3)}{12} \quad (30)$$

We may also consider more complicated cross sections and compute the proper parameters.

Remark 3. We assume that the beam centerline is located in the symmetry plane of the plate, see Fig. 2, which simplifies the modeling of a reinforced plate since it will be subject to pure bending. If the beams are located on one side of the plate the main approach is the same but we must include models for the membrane deformation of the plate and beams.

2.4. The reinforced plate model

Let $S = \{\Sigma\}$ be a set of beams arbitrarily oriented in Ω . Using superposition we obtain the problem: find $u \in V$ such that

$$a(u, v) = l(v) \quad \forall v \in V \quad (31)$$

where

$$V = V_\Omega \bigcap_{\Sigma \in S} V_\Sigma \quad (32)$$

and the forms are defined by

$$a(v, w) = a_\Omega(v, w) + \sum_{\Sigma \in S} a_\Sigma(v, w) \quad (33)$$

$$l(v) = l_\Omega(v) + \sum_{\Sigma \in S} l_\Sigma(v) \quad (34)$$

Remark 4. Note that for the alternative plate reinforcement geometry, right in Fig. 2, there is no geometric error in our method if we use the parameters (30). In the standard reinforcement geometry, left in Fig. 2, there is however a geometric error proportional to b_Σ in the plate bilinear form, which arises in the superposition since the intersection between the beam and the plate is nonempty. We will later see that b_Σ typically is smaller (in practice significantly smaller) than the mesh size since we are using thin beam and plate theory, see (35), and thus the geometric error is small.

3. Finite element discretization

3.1. The mesh and finite element spaces

- We consider a subdivision $\mathcal{T}_h = \{T\}$ of Ω into a geometrically conforming finite element mesh, with mesh parameter $h \in (0, h_0]$. We assume that the elements are shape regular, i.e., the quotient of the diameter of the smallest circumscribed sphere and the largest inscribed sphere is uniformly bounded. We denote by h_T the diameter of element T and by $h = \max_{T \in \mathcal{T}_h} h_T$ the global mesh size parameter.
- Since we are using thin plate and beam theory we assume that there is a constant C_{mesh} such that

$$C_{\text{mesh}} \max(t_\Omega, t_\Sigma, b_\Sigma) \leq h \quad (35)$$

- We shall use continuous, piecewise polynomial approximations, for both the membrane and plate problem. Let

$$V_{\Omega,h,k} = \{v \in C^0(\Omega) : v|_T \in \mathcal{P}_k(T) \forall T \in \mathcal{T}\} \quad (36)$$

where $\mathcal{P}_k(T)$ is the space of polynomials of degree less or equal to k defined on T . For simplicity, we write $V_{\Omega,h} = V_{\Omega,h,k}$.

- To define our method we introduce the set of faces (edges) F in the mesh, $F_h = \{F\}$, and we split F_h into two disjoint subsets

$$F_h = F_{h,I} \cup F_{h,B} \quad (37)$$

where $F_{h,I}$ is the set of faces in the interior of Ω and $F_{h,B}$ is the set of faces on the boundary.

- Further, with each face F we associate a fixed unit normal \mathbf{n}_F such that for faces on the boundary \mathbf{n}_F is the exterior unit normal. We denote the jump of a function \mathbf{v} at a face F by $[\mathbf{v}] = \mathbf{v}^+ - \mathbf{v}^-$ for $F \in F_{h,I}$ and $[\mathbf{v}] = \mathbf{v}^+$ for $F \in F_{h,B}$, and the average $\langle \mathbf{v} \rangle = (\mathbf{v}^+ + \mathbf{v}^-)/2$ for $F \in F_{h,I}$ and $\langle \mathbf{v} \rangle = \mathbf{v}^+$ for $F \in F_{h,B}$, where $\mathbf{v}^\pm = \lim_{\epsilon \downarrow 0} \mathbf{v}(\mathbf{x} \mp \epsilon \mathbf{n}_F)$ with $\mathbf{x} \in F$.
- Given a line segment Σ in Ω that represents a beam we let

$$\mathcal{T}_h(\Sigma) = \{T \in \mathcal{T}_h : T \cap \Sigma \neq \emptyset\}$$

and we let $F_h(\Sigma)$ be the set of all interior faces in $\mathcal{T}_h(\Sigma)$.

- The intersection points between Σ and element faces in $F_h(\Sigma)$ is denoted

$$\mathcal{P}_h(\Sigma) = \{\mathbf{x} : \mathbf{x} = F \cap \Sigma, F \in F_h(\Sigma)\} \quad (38)$$

and we assume that this is a discrete set of points (thus excluding the case where any $F \in F_h$ coincides with a part of Σ), see Fig. 3 for illustration.

Remark 5. The assumption (35) is natural since we use models for thin structures as our basis for the finite element discretization. In particular, in (71) we use the estimate $b_\Sigma \leq Ch$ which means that the mesh size can not become very small in comparison to the beam width. If that would happen the modeling of the beam as a form based on the beam centerline would not be reasonable and a more detailed model should be used as the basis for finite element modeling.

3.2. The c/dG method for the plate

We approximate the solution to the plate problem using the continuous/discontinuous Galerkin (c/dG) method: Find $u_h \in V_{\Omega,h}$, with $k \geq 2$, such that

$$a_{\Omega,h}(u_h, v) = l_\Omega(v) \quad \forall v \in V_{\Omega,h} \quad (39)$$

The bilinear form $a_{\Omega,h}(\cdot, \cdot)$ is defined by

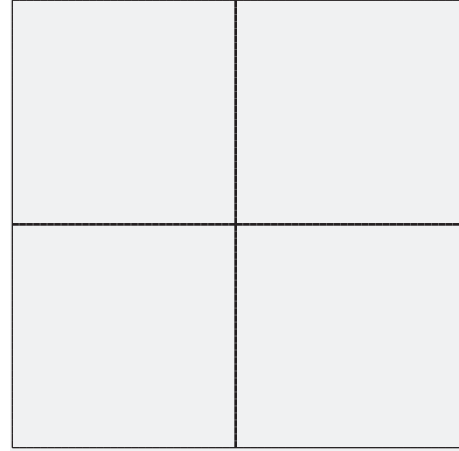


Fig. 4. Beam reinforced plate.

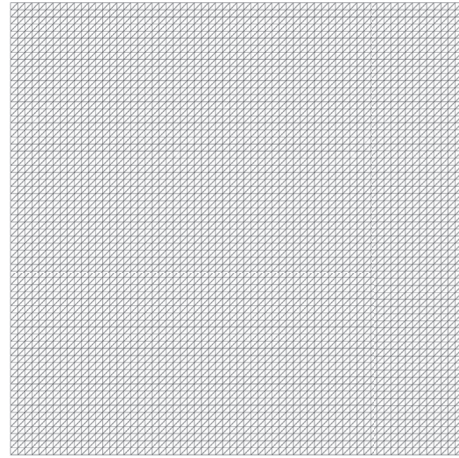


Fig. 5. Computational mesh.

$$\begin{aligned} a_{\Omega,h}(v, w) = & \sum_{T \in \mathcal{T}_h} (\sigma_P(\nabla v), \epsilon(\nabla w))_T \\ & - \sum_{F \in F_{h,I} \cup F_{h,B}} ((\mathbf{n}_F \cdot \sigma_P(\nabla v)), [\nabla w])_F \\ & - \sum_{F \in F_{h,I} \cup F_{h,B}} ([\nabla v], \langle \mathbf{n}_F \cdot \sigma_P(\nabla w) \rangle)_F \\ & + \sum_{F \in F_{h,I} \cup F_{h,B}} \beta_\Omega h_F^{-1} ([\nabla v], [\nabla w])_F \end{aligned} \quad (40)$$

Here β_Ω is a positive parameter of the form

$$\beta_\Omega = \beta_{\Omega,0} C_P = \beta_{\Omega,0} \frac{E_\Omega t_\Omega^3}{12(1 + \nu_\Omega)} \quad (41)$$

where $\beta_{\Omega,0}$ is a constant depending on the polynomial order k , see Ref. [10] for details, and h_F is defined on each face F by

$$h_F = (|T^+| + |T^-|) / (2 |F|) \quad \text{for } F = \partial T^+ \cap \partial T^- \quad (42)$$

with $|T|$ the area of T and $|F|$ the length of F .

Remark 6. The idea of using continuous/discontinuous approximations was first proposed by Engel et al. [6] and later analysed for Kirchhoff–Love and Mindlin–Reissner plates in Refs. [7,9,10], cf. also Wells and Dung [21].

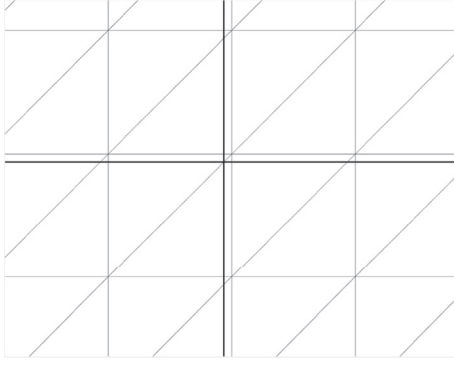


Fig. 6. Beam/mesh intersection at the center.

Remark 7. Other boundary conditions for plates, for instance simply supported and free, can easily be included in the c/dG finite element method, see Ref. [8] for details.

Remark 8. For $v \in V_{\Omega,h}$ we have $[\nabla v] = [\mathbf{n}_F \cdot \nabla v] \mathbf{n}_F$ since v is continuous across a face and $v = 0$ on $\partial\Omega$. Therefore

$$([\mathbf{n}_F \cdot \sigma(\nabla v)], [\nabla w])_F = ([\mathbf{n}_F \cdot \sigma(\nabla v)] \cdot \mathbf{n}_F, [\mathbf{n}_F \cdot \nabla w])_F \quad (43)$$

for all $v, w \in V_{\Omega,h}$, and we note that $(\mathbf{n}_F \cdot \sigma(\nabla v) \cdot \mathbf{n}_F)|_F$ is the bending moment at the edge F .

3.3. The cut c/dG method for a beam

We propose the following cut c/dG method. Find $u_h \in V_{\Sigma,h} = V_{\Omega,h}|_{\mathcal{T}_h(\Sigma)}$ such that

$$A_{\Sigma,h}(u_h, v) = l_{\Sigma}(v) \quad \forall v \in V_{\Sigma,h} \quad (44)$$

where the forms are defined by

$$A_{\Sigma,h}(v, w) = a_{\Sigma,h}(v, w) + s_{\Sigma,h}(v, w) \quad (45)$$

$$\begin{aligned} a_{\Sigma,h}(v, w) &= \sum_{T \in \mathcal{T}_h(\Sigma)} (\sigma_{B,\Sigma}(\nabla_{\Sigma} v), \epsilon(\nabla_{\Sigma} w))_{\Sigma \cap T} \\ &\quad - \sum_{x \in \mathcal{P}_h(\Sigma)} (\langle \mathbf{t} \cdot \sigma_{B,\Sigma}(\nabla_{\Sigma} v) \rangle, [\nabla_{\Sigma} w])_x \\ &\quad - \sum_{x \in \mathcal{P}_h(\Sigma)} ([\nabla_{\Sigma} v], \langle \mathbf{t} \cdot \sigma_{B,\Sigma}(\nabla_{\Sigma} w) \rangle)_x \\ &\quad + \sum_{x \in \mathcal{P}_h(\Sigma)} \beta_{\Sigma} h^{-1} ([\nabla_{\Sigma} v], [\nabla_{\Sigma} w])_x \end{aligned} \quad (46)$$

$$\begin{aligned} s_{\Sigma,h}(v, w) &= \sum_{F \in \mathcal{F}_h(\Sigma)} \sum_{j=0}^k \sum_{i=0}^2 h^{2j} \| [\partial_{\mathbf{n}_F}^j \partial_{\mathbf{t}_F}^i v] \|_F^2 \\ &\quad + \sum_{T \in \mathcal{T}_h(\Sigma)} \sum_{i=0}^2 \gamma_{\Sigma,2} h (\partial_{\mathbf{n}_{\Sigma}} \partial_{\mathbf{t}_{\Sigma}}^i v, \partial_{\mathbf{n}_{\Sigma}} \partial_{\mathbf{t}_{\Sigma}}^i w)_T \end{aligned} \quad (47)$$

Here we used the notation $(v, w)_x = v(x)w(x)$, the penalty parameter takes the form

$$\beta_{\Sigma} = \beta_{\Sigma,0} C_B = \beta_{\Sigma,0} E_{\Sigma} I_{\Sigma} \quad (48)$$

with $\beta_{\Sigma,0}$ a parameter that only depends on the polynomial order, and $s_{\Sigma,h}$ is a stabilization form with positive parameters

$$\gamma_{\Sigma,i} = \gamma_{\Sigma,i,0} C_B = \gamma_{\Sigma,i,0} E_{\Sigma} I_{\Sigma}, \quad i = 1, 2 \quad (49)$$

The form $s_{\Sigma,h}$ is added to ensure coercivity and stability of the stiffness matrix, cf. [1], in the case when the beam is not embedded in a plate

or if the plate is very weak. For completeness we provide an analysis of this case, which also motivates the form of the stabilization form, in Appendix A below.

Remark 9. Using the identities

$$\nabla_{\Sigma} v = (\partial_{\mathbf{t}} v) \mathbf{t}, \quad \epsilon_{\Sigma}(\nabla_{\Sigma} v) = (\partial_{\mathbf{t}}^2 v) \mathbf{t} \otimes \mathbf{t}, \quad \sigma_{B,\Sigma}(\nabla_{\Sigma} v) = E_{\Sigma} I_{\Sigma} (\partial_{\mathbf{t}}^2 v) \mathbf{t} \otimes \mathbf{t} \quad (50)$$

we note that $a_{\Sigma,h}$ can alternatively be written in the form

$$\begin{aligned} a_{\Sigma,h}(v, w) &= \sum_{T \in \mathcal{T}_h(\Sigma)} (E_{\Sigma} I_{\Sigma} \partial_{\mathbf{t}}^2 v, \partial_{\mathbf{t}}^2 w)_{\Sigma \cap T} \\ &\quad - \sum_{x \in \mathcal{P}_h(\Sigma)} (\langle E_{\Sigma} I_{\Sigma} \partial_{\mathbf{t}}^2 v \rangle, [\partial_{\mathbf{t}} w])_x \\ &\quad - \sum_{x \in \mathcal{P}_h(\Sigma)} ([\partial_{\mathbf{t}} v], \langle E_{\Sigma} I_{\Sigma} \partial_{\mathbf{t}}^2 w \rangle)_x \\ &\quad + \sum_{x \in \mathcal{P}_h(\Sigma)} \frac{\beta_{\Sigma,0}}{h} (E_{\Sigma} I_{\Sigma} [\partial_{\mathbf{t}} v], [\partial_{\mathbf{t}} w])_x \end{aligned} \quad (51)$$

which is the form in Ref. [6].

Remark 10. The terms on the discrete set $\mathcal{P}_h(\Sigma)$ are associated with the work of the end moments on the end rotation which occur due to the lack of $C^1(\Omega)$ continuity of the approximation, as in the plate model. See Remark 8.

Remark 11. We note that due to the stabilization this method works for a single beam, i.e. without being embedded in a plate. The basic principle is the same as for the trace finite element method proposed in Ref. [18] and the stabilized version proposed in Ref. [2]. When the beam is embedded in a plate, which is the case in this work, the need for the stabilization term is mitigated, and if the plate is sufficiently stiff we may omit the stabilization term, see Section 3.5 for further details.

3.4. The c/dG method for the reinforced plate model

Recall that $S = \{\Sigma\}$ is a set of beams arbitrarily oriented in Ω . Using superposition we obtain the problem: find $u_h \in V_{\Omega,h}$ such that

$$A_h(u_h, v) = l(v) \quad \forall v \in V_{\Omega,h} \quad (52)$$

where the forms are defined by

$$A_h(v, w) = a_{\Omega,h}(v, w) + \sum_{\Sigma \in S} a_{\Sigma,h}(v, w) \quad (53)$$

$$l(v) = l_{\Omega}(v) + \sum_{\Sigma \in S} l_{\Sigma}(v) \quad (54)$$

3.5. Coercivity for reinforced plates

In this section we study the coercivity of the c/dG method for the reinforced plate. We shall use the stability provided by the plate to prove stability of the reinforced plate, without the need of the stabilizing terms ($\gamma_{\Sigma,1} = \gamma_{\Sigma,2} = 0$). This is only possible as long as the mesh size h is larger than or equal to the beam with b_{Σ} . When this condition is not satisfied, stability uniform in h is achieved only when the stabilizing terms are included ($\gamma_{\Sigma,1}, \gamma_{\Sigma,2} > 0$), using similar ideas as in Refs. [2,3].

Coercivity of the Plate. We first recall that the c/dG method for the plate is coercive. Introducing the energy norm

$$\|v\|_{\Omega,h}^2 = \sum_{T \in \mathcal{T}_h} C_P \|\nabla^2 v\|_T^2 + \sum_{F \in \mathcal{F}_h} C_P h \|\langle \nabla^2 v \rangle\|_F^2 + \sum_{F \in \mathcal{F}_h} C_P h^{-1} \|[\nabla v]\|_F^2 \quad (55)$$

there is a constant $m_p > 0$ such that

$$m_p \|v\|_{\Omega,h}^2 \leq a_{\Omega,h}(v, v) \quad \forall v \in V_{\Omega,h} \quad (56)$$

for β_{Ω} large enough.

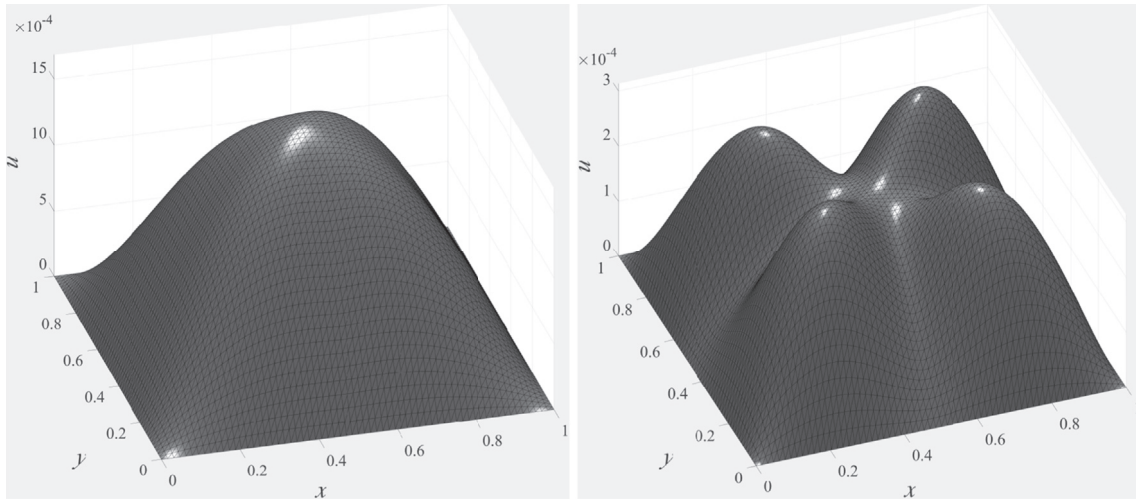


Fig. 7. Displacements using simply supported support for the beams, $E_\Sigma = 100E_\Omega$ (left) and $E_\Sigma = 1000E_\Omega$ (right).

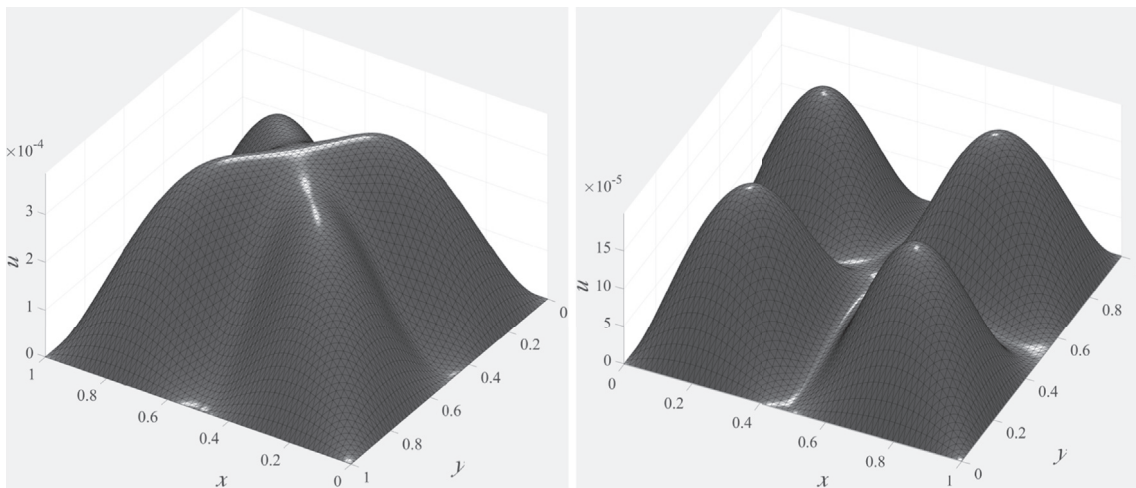


Fig. 8. Displacements using fixed support for the beams, $E_\Sigma = 100E_\Omega$ (left) and $E_\Sigma = 1000E_\Omega$ (right).

Coercivity of the Reinforced Plate. Next turning to the reinforced plate we introduce the energy norm associated with the beam

$$\begin{aligned} \|v\|_{\Sigma,h}^2 &= \sum_{T \in \mathcal{T}_h(\Sigma)} C_B \|\partial_t^2 v\|_{\Sigma \cap T}^2 + \sum_{x \in \mathcal{P}_h(\Sigma)} C_B h \|\langle \partial_t^2 v \rangle_x\|_x^2 \\ &\quad + \sum_{x \in \mathcal{P}_h(\Sigma)} C_B h^{-1} \|[\partial_t v]\|_x^2 \end{aligned} \quad (57)$$

Then there is a constant m such that

$$m \left(\|v\|_{\Sigma,h}^2 + \|v\|_{\Omega,h}^2 \right) \lesssim A_h(v, v) \quad \forall v \in V_h \quad (58)$$

for β_Ω and β_Σ large enough.

Verification of (58). Using the following two inequalities, which we verify below,

$$C_1 \left(\sum_{x \in \mathcal{P}_h(\Sigma)} C_B h \|\langle \partial_t^2 v \rangle_x\|_x^2 \right) \leq \sum_{T \in \mathcal{T}_h} C_P \|\nabla^2 v\|_T^2 \quad (59)$$

for some constant $C_1 > 0$, and

$$\begin{aligned} \sum_{T \in \mathcal{T}_h(\Sigma)} C_B \|\partial_t^2 v\|_{\Sigma \cap T}^2 + \sum_{x \in \mathcal{P}_h(\Sigma)} C_B h^{-1} \|[\partial_t v]\|_x^2 \\ \leq \sum_{T \in \mathcal{T}_h} \frac{m_P}{3} C_P \|\nabla^2 v\|_T^2 + a_{\Sigma,h}(v, v) \end{aligned} \quad (60)$$

for β_Σ large enough, we have

$$A_h(v, v) = a_{\Omega,h}(v, v) + a_{\Sigma,h}(v, v) \quad (61)$$

$$\geq m_P \|v\|_{\Omega,h}^2 + a_{\Sigma,h}(v, v) \quad (62)$$

$$= \frac{m_P}{3} \|v\|_{\Omega,h}^2 + \frac{m_P}{3} \|v\|_{\Omega,h}^2 + \left(\frac{m_P}{3} \|v\|_{\Omega,h}^2 + a_{\Sigma,h}(v, v) \right) \quad (63)$$

$$\geq \frac{m_P}{3} \|v\|_{\Omega,h}^2 + \frac{C_1 m_P}{3} \left(\sum_{x \in \mathcal{P}_h(\Sigma)} C_B h \|\langle \partial_t^2 v \rangle_x\|_x^2 \right) \quad (64)$$

$$\begin{aligned} &+ \left(\sum_{T \in \mathcal{T}_h(\Sigma)} C_B \|\partial_t^2 v\|_{\Sigma \cap T}^2 + \sum_{x \in \mathcal{P}_h(\Sigma)} C_B h^{-1} \|[\partial_t v]\|_x^2 \right) \\ &\geq m \left(\|v\|_{\Sigma,h}^2 + \|v\|_{\Omega,h}^2 \right) \end{aligned} \quad (65)$$

where $m = \min(m_P/3, C_1 m_P/3)$.

Verification of (59). We note that, for a point $x \in \Sigma \cap T$, $T \in \mathcal{T}_h$, we have the estimates

$$\|\partial_t^2 v\|_x \leq C_{\text{inv}} h^{-1} \|\partial_t^2 v\|_T \leq C_{\text{inv}} h^{-1} \|\nabla^2 v\|_T \quad (66)$$

where used the fact that \mathbf{t} is a constant unit vector so that $\partial_{\mathbf{t}}^2 v = \mathbf{t} \cdot (\nabla^2 v) \cdot \mathbf{t} \in \mathcal{P}_{k-2}(T)$ is a well defined expression on T since $v \in \mathcal{P}_k(T)$ is a polynomial on T then we used an inverse inequality to pass from the point value to the L^2 norm on the element T . For instance, in the important case of quadratic elements $\nabla^2 v$ is a constant and for a constant function w we have the estimate

$$\|w\|_{\mathbf{x}}^2 = w^2(\mathbf{x}) = |T|^{-1} |T| w^2(\mathbf{x}) = |T|^{-1} \|w\|_T^2 \lesssim h^{-2} \|w\|_T^2 \quad (67)$$

since it follows from shape regularity of T and quasiuniformity of the mesh that the element area $|T| \sim h^2$.

Using (66) we obtain, with $\mathcal{T}_h(\mathbf{x}) = \{T \in \mathcal{T}_h : \mathbf{x} \in \bar{T}\}$ the set of all elements such that $\mathbf{x} \in \bar{T}$,

$$\sum_{\mathbf{x} \in \mathcal{P}_h(\Sigma)} C_B h \|\langle \partial_{\mathbf{t}}^2 v \rangle\|_{\mathbf{x}}^2 \leq \sum_{\mathbf{x} \in \mathcal{P}_h(\Sigma)} C_{\text{inv}}^2 \frac{C_B}{C_P h} C_P \|\nabla^2 v\|_{\mathcal{T}_h(\mathbf{x})}^2 \quad (68)$$

$$\leq C_{\text{inv}}^2 \frac{C_B}{C_P h} \|v\|_{\Omega, h}^2 \quad (69)$$

and thus we have the estimate

$$\underbrace{\frac{1}{C_{\text{inv}}^2} \frac{C_P h}{C_B}}_{C_1} \left(\sum_{\mathbf{x} \in \mathcal{P}_h(\Sigma)} C_B h \|\langle \partial_{\mathbf{t}}^2 v \rangle\|_{\mathbf{x}}^2 \right) \leq \|v\|_{\Omega, h}^2 \quad (70)$$

We note, using the definitions (4) and (24) of C_P and C_B , that

$$\frac{C_P h}{C_B} = \frac{1}{1 + \nu_{\Omega}} \frac{E_{\Omega} t_{\Omega}^3}{E_{\Sigma} t_{\Sigma}^3} \frac{h}{b_{\Sigma}} \geq \frac{1}{1 + \nu_{\Omega}} \frac{E_{\Omega} t_{\Omega}^3}{E_{\Sigma} t_{\Sigma}^3} C_{\text{mesh}} \quad (71)$$

where we used the condition that the beam width is smaller than the mesh size (35) and thus the right hand side is a positive constant independent of the mesh size and so is C_1 .

Verification of (60). First we have the equality

$$\begin{aligned} a_{\Sigma, h}(v, v) &= \sum_{T \in \mathcal{T}_h(\Sigma)} C_B \|\partial_{\mathbf{t}}^2 v\|_{\Sigma \cap T}^2 \\ &\quad - 2 \underbrace{\sum_{\mathbf{x} \in \mathcal{P}_h(\Sigma)} C_B \langle \langle \partial_{\mathbf{t}}^2 v \rangle, [\partial_{\mathbf{t}} v] \rangle_{\mathbf{x}}}_{\star} \\ &\quad + \sum_{\mathbf{x} \in \mathcal{P}_h(\Sigma)} \beta_{\Sigma, 0} C_B h^{-1} \|[\partial_{\mathbf{t}} v]\|_{\mathbf{x}}^2 \end{aligned} \quad (72)$$

To estimate \star we employ the inverse inequality (66) as follows

$$\star = 2 \sum_{\mathbf{x} \in \mathcal{P}_h(\Sigma)} C_B \langle \langle \partial_{\mathbf{t}}^2 v \rangle, [\partial_{\mathbf{t}} v] \rangle_{\mathbf{x}} \quad (73)$$

$$\leq 2 \sum_{\mathbf{x} \in \mathcal{P}_h(\Sigma)} C_B C_{\text{inv}} h^{-1} \|\nabla^2 v\|_{\mathcal{T}_h(\mathbf{x})} \|[\partial_{\mathbf{t}} v]\|_{\mathbf{x}} \quad (74)$$

$$\begin{aligned} &\leq \sum_{T \in \mathcal{T}_h(\Sigma)} \delta C_B C_{\text{inv}}^2 h^{-1} \|\nabla^2 v\|_T^2 \\ &\quad + \sum_{\mathbf{x} \in \mathcal{P}_h(\Sigma)} \delta^{-1} C_B h^{-1} \|[\partial_{\mathbf{t}} v]\|_{\mathbf{x}}^2 \end{aligned} \quad (75)$$

where we used the inequality $ab \leq (\delta a^2 + \delta^{-1} b^2)/2$ for $\delta > 0$. We then obtain (60) as follows

$$\begin{aligned} \sum_{T \in \mathcal{T}_h} \frac{m_P}{3} C_P \|\nabla^2 v\|_T^2 + a_{\Sigma, h}(v, v) &\geq \sum_{T \in \mathcal{T}_h(\Sigma)} C_B \|\partial_{\mathbf{t}}^2 v\|_{\Sigma \cap T}^2 \\ &\quad + \underbrace{\sum_{T \in \mathcal{T}_h} \left(\frac{m_P}{3} C_P - \delta C_B C_{\text{inv}}^2 h^{-1} \right)}_{\geq 0} \|\nabla^2 v\|_T^2 \\ &\quad + \underbrace{\sum_{\mathbf{x} \in \mathcal{P}_h(\Sigma)} (\beta_{\Sigma, 0} - \delta^{-1}) C_B h^{-1}}_{\geq 1} \|[\partial_{\mathbf{t}} v]\|_{\mathbf{x}}^2 \end{aligned} \quad (76)$$

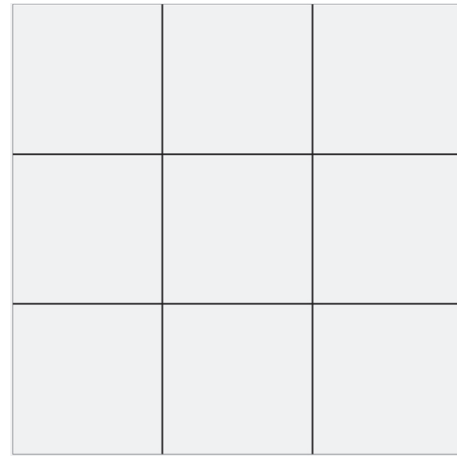


Fig. 9. Beam reinforced plate.

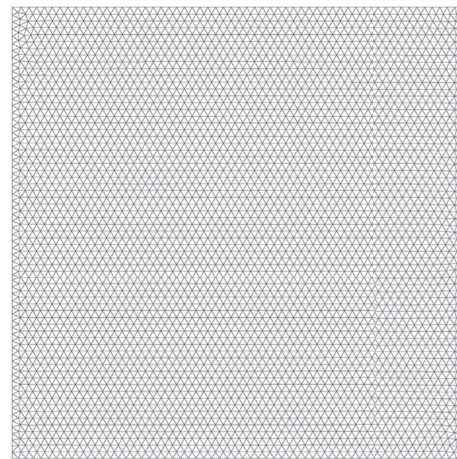


Fig. 10. Computational mesh.

$$\geq \sum_{\mathbf{x} \in \mathcal{P}_h(\Sigma)} C_B h^{-1} \|[\partial_{\mathbf{t}} v]\|_{\mathbf{x}}^2 + \sum_{\mathbf{x} \in \mathcal{P}_h(\Sigma)} C_B h^{-1} \|[\partial_{\mathbf{t}} v]\|_{\mathbf{x}}^2 \quad (77)$$

Here we choose: δ small enough to guarantee that

$$\begin{aligned} 0 \leq \frac{m_P}{3} C_P - \delta C_B C_{\text{inv}}^2 h^{-1} &= \frac{m_P}{3} C_P \left(1 - \delta \frac{3}{m_P} \frac{C_B C_{\text{inv}}^2}{C_P h} \right) \\ &= \frac{m_P}{3} C_P \left(1 - \delta \frac{3}{m_P} \frac{1}{C_1} \right) \end{aligned} \quad (78)$$

where as above, see (71), $C_1 > 0$ independent of the mesh parameter h , and β_{Σ} such that

$$\beta_{\Sigma} - \frac{1}{\delta} \geq 1 \quad (79)$$

4. Numerical examples

In this section, we give some elementary examples of what can be achieved with the presented technique. In all numerical examples we use polynomial order 2, $f_{\Sigma} = 0$, and

$$f_{\Omega} = 8C_P(3(x^2(1-x)^2 + y^2(1-y)^2) + (1-6x(1-x))(1-6y(1-y)))$$

corresponding to the solution $u = x^2(1-x)^2y^2(1-y)^2$ for a clamped plate unsupported by beams.

In order to handle more general boundary conditions we in particular need to be able to impose end displacements on the beam in the

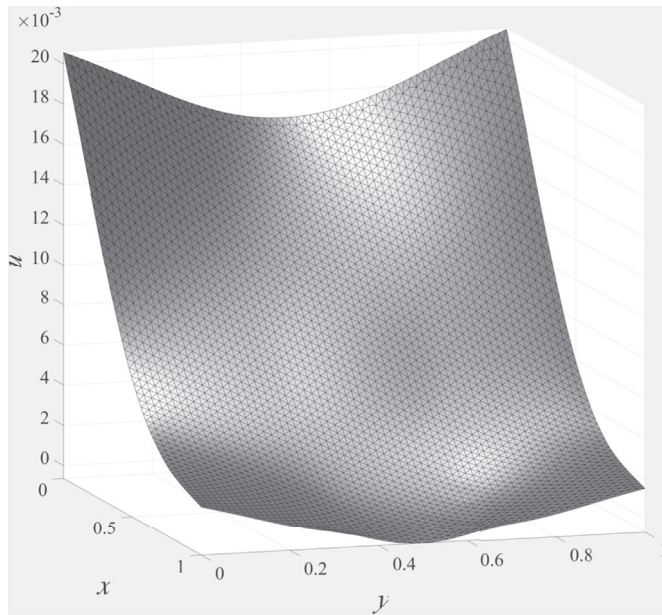


Fig. 11. Deformations when the beams are clamped at $x = 1$.

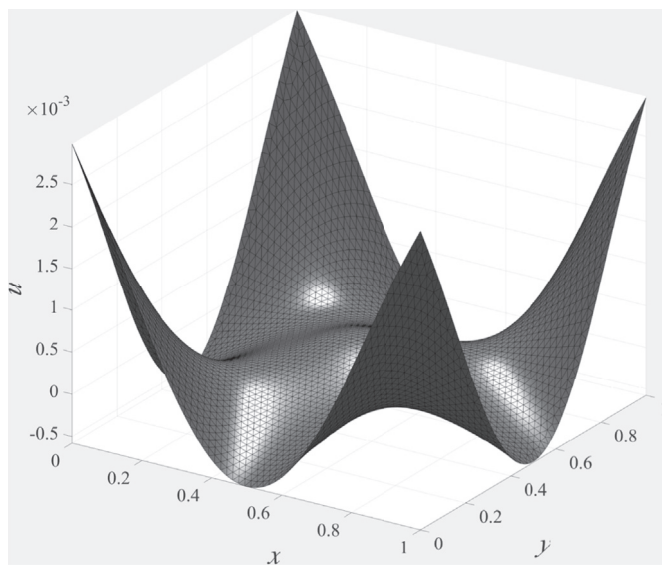


Fig. 12. Deformations when all beams are clamped.

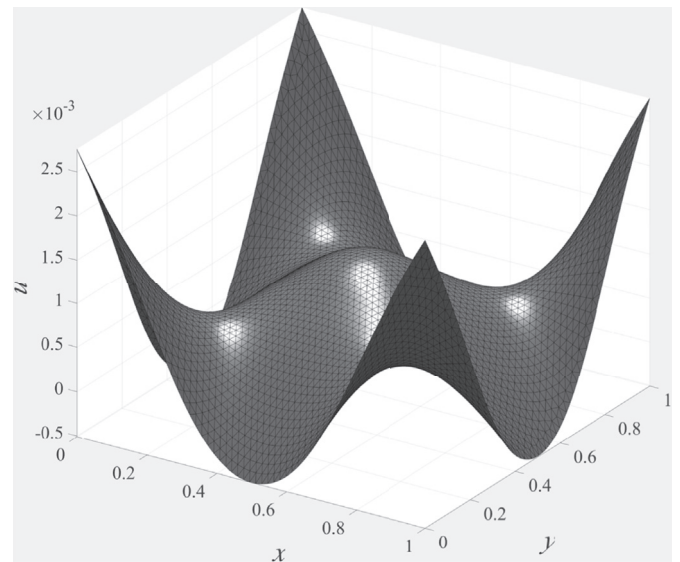


Fig. 13. Deformations when all beams are simply supported.

thickness $t_\Omega = 0.1$. The plate is supported by two beams oriented as in Fig. 4, one at $x = 0.499$ and one at $y = 0.499$ (to avoid intersection with the mesh lines). The computational mesh is shown in Fig. 5 and in Fig. 6 were show a close-up of the intersection between the beams and the mesh.

For this problem we test two different supports for the beams: simply supported and fixed, and two different stiffnesses for the beams: $E_\Sigma = 100E_\Omega$ and $E_\Sigma = 1000E_\Omega$. The thickness and width of the beam are equal and the same as the thickness of the plate. In Fig. 7 we show the results using $E_\Sigma = 100E_\Omega$, with simply supported and fixed supports; in Fig. 8 we show the results using $E_\Sigma = 1000E_\Omega$, with simply supported and fixed supports.

4.2. Plate only supported by beams

Next, we consider a plate with free boundaries, supported only by beams. All data for the plate are the same as in the previous example. The plate is supported by four beams positioned at $1/3$ and $2/3$ from each boundary as indicated in Fig. 9. The beams have the same dimension as previously, with Young’s modulus $E_\Sigma = 100E_\Omega$. The computational mesh is unstructured and shown in Fig. 10.

We first consider the case when the beams are clamped at $x = 1$ and free elsewhere. In Fig. 11 we see an elevation of the corresponding deformation. Next we consider the case when all beams are clamped, Fig. 12, and simply supported, Fig. 13. Note the slight increase in central displacement for the latter.

5. Conclusions

We have formulated a continuous/discontinuous Galerkin method for beam reinforced thin plates. The method has the advantage that we can discretize both the beam and plate problem with the same standard finite element spaces of continuous piecewise polynomials defined on triangles (or quadrilaterals).

Acknowledgement

This research was supported in part by the Swedish Foundation for Strategic Research Grant No. AM13-0029, the Swedish Research Council Grant No. 2013-4708, and the Swedish strategic research programme eSSENCE. The first author was supported in part by EPSRC grant EP/P01576X/1.

case of a free plate (we note that strongly imposed boundary conditions on the plate are also enforced on the beam). Zero displacement of the beam endpoints \mathbf{x}_E are imposed by adding penalty terms

$$\frac{\tilde{\beta}_{\Sigma,0}}{h^3} (E_\Sigma I_\Sigma v, w)_{\mathbf{x}_E} \tag{80}$$

to the form $a_{\Sigma,h}(v, w)$ in (51), where $\tilde{\beta}_{\Sigma,0}$ is a penalty parameter. These terms suffice for optimal order convergence (of the beam approximation) in the case of second degree polynomial approximations since the shear forces required for energy consistency are third derivatives of displacements, and thus equal zero.

4.1. Simply supported plate using beams with different supports

We consider a simply supported plate on the domain $\Omega = (0, 1) \times (0, 1)$ with Young’s modulus $E_\Omega = 100$, Poisson’s ratio $\nu_\Omega = 1/2$, and

Appendix A. Coercivity for beams which are not embedded in a plate

To prove coercivity of the bilinear form associated with the beam $A_{\Sigma,h}$, defined in (45), in the case when the beam is not embedded in a plate we utilize the stabilization term $s_{\Sigma,h}$, see (47), which provides the following estimate

$$\sum_{T \in \mathcal{T}_h(\Sigma)} \sum_{j=0}^2 C_B h^{-1} \|\partial_t^j v\|_T^2 \leq C_{\text{stab}} \left(\sum_{j=0}^2 C_B \|\partial_t^2 v\|_{\Sigma}^2 + \|v\|_{s_{\Sigma,h}}^2 \right) \quad (\text{A.1})$$

where $\|v\|_{s_{\Sigma,h}}^2 = s_{\Sigma,h}(v, v)$. Starting from (72) we use the first inequality in (66) followed by (A.2) to estimate \star as follows

$$\star = 2 \sum_{x \in \mathcal{P}_h(\Sigma)} C_B \langle \partial_t^2 v, [\partial_t v]_x \rangle \quad (\text{A.2})$$

$$\leq 2 \sum_{x \in \mathcal{P}_h(\Sigma)} C_B C_{\text{inv}} h^{-1} \|\partial_t^2 v\|_{\mathcal{T}_h(x)} \|[\partial_t v]\|_x \quad (\text{A.3})$$

$$\leq \sum_{T \in \mathcal{T}_h(\Sigma)} \delta C_B C_{\text{inv}}^2 h^{-1} \|\partial_t^2 v\|_T^2 + \sum_{x \in \mathcal{P}_h(\Sigma)} \delta^{-1} C_B h^{-1} \|[\partial_t v]\|_x^2 \quad (\text{A.4})$$

$$\leq \delta C_{\text{inv}}^2 C_{\text{stab}} \left(\sum_{T \in \mathcal{T}_h(\Sigma)} C_B \|\partial_t^2 v\|_{\Sigma \cap T}^2 + \|v\|_{s_{\Sigma,h}}^2 \right) + \sum_{x \in \mathcal{P}_h(\Sigma)} \delta^{-1} C_B h^{-1} \|[\partial_t v]\|_x^2 \quad (\text{A.5})$$

Now choosing δ small enough and $\beta_{\Sigma,0}$ large enough we obtain the coercivity estimate

$$\sum_{T \in \mathcal{T}_h(\Sigma)} C_B \|\partial_t^2 v\|_{\Sigma \cap T}^2 + \|v\|_{s_{\Sigma,h}}^2 + \sum_{x \in \mathcal{P}_h(\Sigma)} C_B h \|\langle \partial_t^2 v \rangle\|_x^2 + \sum_{x \in \mathcal{P}_h(\Sigma)} C_B h^{-1} \|[\partial_t v]\|_x^2 \lesssim A_{\Sigma,h}(v, v) \quad (\text{A.6})$$

for all $v \in V_{\Sigma,h}$. For completeness we include the main steps in the derivation of (A.1). For related results we refer to [3] and [14].

- For an element T with a so called large intersection with Σ , that is $|T \cap \Sigma| \gtrsim$, it holds, for $v \in \mathcal{P}_k(T)$,

$$\|v\|_T^2 \lesssim h \|v\|_{T \cap \Sigma}^2 + h^2 \|\partial_{n_\Sigma} v\|_F^2 \quad (\text{A.7})$$

Setting $v = \partial_t^i w$, $i = 0, 1, 2$, we get

$$\sum_{i=0}^2 h^{-1} \|\partial_t^i w\|_T^2 \lesssim \|\partial_t^i w\|_{T \cap \Sigma}^2 + \sum_{i=0}^2 h \|\partial_{n_\Sigma} \partial_t^i w\|_F^2 \quad (\text{A.8})$$

- For two elements T_1 and T_2 which share the face F it holds, for all $w_1 \in \mathcal{P}_k(T_1)$ and $w_2 \in \mathcal{P}_k(T_2)$,

$$\|w_1\|_{T_1}^2 \lesssim \|w_2\|_{T_2}^2 + \sum_{j=0}^k h^{2j+1} \|[\partial_{n_F}^j w]\|_F^2 \quad (\text{A.9})$$

see Ref. [12]. Setting $w = \partial_t^i v$, $i = 0, 1, 2$, we obtain

$$\sum_{i=0}^2 h^{-1} \|\partial_t^i v\|_{T_1}^2 \lesssim \sum_{i=0}^2 h^{-1} \|\partial_t^i v\|_{T_2}^2 + \sum_{j=0}^k \sum_{i=0}^2 h^{2j} \|[\partial_{n_F}^j \partial_t^i v]\|_F^2 \quad (\text{A.10})$$

- To prove the stability estimate (A.1) we note that it follows from quasi uniformity that for each element $T \in \mathcal{T}_h(\Sigma)$ there is a path of elements $\{T_i\}_{i=0}^n$, with length n uniformly bounded, such that $T_0 = T$, T_i and T_{i+1} share a face, and T_n has a large intersection with Σ . Using (A.10) to pass between the elements in the path and then finally using (A.8) we obtain (A.1).

References

- [1] E. Burman, S. Claus, P. Hansbo, M.G. Larson, A. Massing, CutFEM: discretizing geometry and partial differential equations, *Int. J. Numer. Meth. Eng.* 104 (7) (2015) 472–501.
- [2] E. Burman, P. Hansbo, M.G. Larson, A stabilized cut finite element method for partial differential equations on surfaces: the Laplace-Beltrami operator, *Comput. Meth. Appl. Mech. Eng.* 285 (2015) 188–207.
- [3] E. Burman, P. Hansbo, M.G. Larson, A. Massing, Cut finite element methods for partial differential equations on embedded manifolds of arbitrary codimensions, *ArXiv e-prints* (Oct. 2016).
- [4] M. Cenanovic, P. Hansbo, M.G. Larson, Cut finite element modeling of linear membranes, *Comput. Meth. Appl. Mech. Eng.* 310 (2016) 98–111.
- [5] A. Deb, M. Booton, Finite element models for stiffened plates under transverse loading, *Comput. Struct.* 28 (3) (1988) 361–372.
- [6] G. Engel, K. Garikipati, T.J.R. Hughes, M.G. Larson, L. Mazzei, R.L. Taylor, Continuous/discontinuous finite element approximations of fourth-order elliptic problems in structural and continuum mechanics with applications to thin beams and plates and strain gradient elasticity, *Comput. Meth. Appl. Mech. Eng.* 191 (34) (2002) 3669–3750.
- [7] P. Hansbo, D. Heintz, M.G. Larson, A finite element method with discontinuous rotations for the Mindlin-Reissner plate model, *Comput. Meth. Appl. Mech. Eng.* 200 (5–8) (2011) 638–648.
- [8] P. Hansbo, M.G. Larson, A discontinuous Galerkin method for the plate equation, *Calcolo* 39 (1) (2002) 41–59.

- [9] P. Hansbo, M.G. Larson, A P^2 -continuous, P^1 -discontinuous finite element method for the Mindlin-Reissner plate model, in: F. Brezzi, A. Buffa, S. Corsaro, A. Muri (Eds.), *Numerical Mathematics and Advanced Applications*, Springer Italia, Milan, 2003, pp. 765–774.
- [10] P. Hansbo, M.G. Larson, A posteriori error estimates for continuous/discontinuous Galerkin approximations of the Kirchhoff-Love plate, *Comput. Meth. Appl. Mech. Eng.* 200 (47–48) (2011) 3289–3295.
- [11] P. Hansbo, M.G. Larson, K. Larsson, Variational formulation of curved beams in global coordinates, *Comput. Mech.* 53 (4) (2014) 611–623.
- [12] P. Hansbo, M.G. Larson, K. Larsson, Cut finite element methods for linear elasticity problems, *ArXiv e-prints* (2017) abs/1703.04377.
- [13] T. Holopainen, Finite element free vibration analysis of eccentrically stiffened plates, *Comput. Struct.* 56 (6) (1995) 993–1007.
- [14] M.G. Larson, S. Zahedi, Stabilization of higher order cut finite element methods on surfaces, *ArXiv e-prints* (Oct. 2017).
- [15] B. Lé, G. Legrain, N. Moës, Mixed dimensional modeling of reinforced structures, *Finite Elem. Anal. Des.* 128 (2017) 1–18.
- [16] A. Mukherjee, M. Mukhopadhyay, Finite element free vibration of eccentrically stiffened plates, *Comput. Struct.* 30 (6) (1988) 1303–1317.
- [17] J.R. O’Leary, I. Harari, Finite element analysis of stiffened plates, *Comput. Struct.* 21 (5) (1985) 973–985.
- [18] M.A. Olshanskii, A. Reusken, J. Grande, A finite element method for elliptic equations on surfaces, *SIAM J. Numer. Anal.* 47 (5) (2009) 3339–3358.
- [19] G. Palani, N.R. Iyer, T. Appa Rao, An efficient finite element model for static and vibration analysis of plates with arbitrarily located eccentric stiffeners, *J. Sound Vib.* 166 (3) (1993) 409–427.
- [20] M. Rossow, A. Ibrahimkhail, Constraint method analysis of stiffened plates, *Comput. Struct.* 8 (1) (1978) 51–60.
- [21] G.N. Wells, N.T. Dung, A C^0 discontinuous Galerkin formulation for Kirchhoff plates, *Comput. Meth. Appl. Mech. Eng.* 196 (35–36) (2007) 3370–3380.